Designing of Copper Nanoparticle Size Formed *via* Aerosol Pyrolysis

VUKOMAN JOKANOVIĆ, BOŽANA ČOLOVIĆ, SREĆKO STOPIĆ, and BERND FRIEDRICH

In this article, the synthesis and structural design of spherical, nonagglomerated particles of copper powder, synthesized by ultrasonic atomization of copper sulfate solutions in hydrogen atmosphere at 1173 K (900 °C), was investigated. Well-controlled particle sizes of Cu powders were obtained from precursor solutions of various concentrations. The mean particle diameters and the ranges of particle size distribution were investigated by scanning electron microscopy (SEM). The diameter values of Cu particles obtained experimentally and estimated theoretically, using the most frequently applied atomization models, were compared. Special attention was paid to our break up capillary waves model, described elsewhere and significantly advanced by Jokanović's theoretical approach, which was applied for the first time to a copper metal system as described in this article. The best agreement between the calculated and the experimentally obtained values was found using this model.

I. INTRODUCTION

TODAY, submicron and micron particles of copper are industrially produced either from copper sulfate solutions by electrolytic recovery[1] or by hydrogen reduction under high pressure in an autoclave.[2] In the hydrocopper process, copper sulfate is reduced by hydrogen at a temperature of 448 K (175 °C) and pressure of 25 bar.[2] Previous experimental and theoretical studies have shown very good mechanical and catalytic properties of so-obtained nanostructured copper powders,[3] which in many applications, as shown elsewhere, are vastly superior to bulk copper materials. This probably results from their fine grain size and enhanced specific surface areas. There are, of course, some drawbacks related to difficulties in preparation of powders without thin oxide layers, which are frequently formed immediately after their exposure to air, even in the cases of very low concentrations of oxygen during powder fabrication.

The application of copper nanoparticles of diameters in the range 0.1 to 1000 nm in preparation of drugs for delaying senility and treating cerebral ischemia and cerebral thrombus squeal is well known. Its main advantages are a curative effect and high levels of safety. The use of copper in interconnection of integrated circuits is one example of amazing copper applications in nanotechnology. Today, the dominant application of copper nanopowders is in catalysis. Although gold nanoparticles show the highest catalytic activity, the advantages of nanocopper are significant; its reactivity is similar to that of nanogold and its price is much lower. Chemical reactions catalyzed by fine copper powders, such as copper powders obtained by ultrasonic spray pyrolysis, exhibit faster kinetics and can be carried out at temperatures lower than those when coarse powders are used. Copper nanoparticles can be used in organic synthesis reactions, like the oxidation of phenol with molecular oxygen,[4] oxidation of alkanethiols,[5] coupling of epoxyalkylhalides,[6] and in the Ullmann reaction.[7] Also, the Cu nanoparticles enhance the catalytic activity and selectivity of ZnO in hydration, dehydration, and hydrogenation reactions in methanol synthesis.[8]

The ultrasonic spray pyrolysis (USP) is an innovative, powerful tool for the synthesis of particles of various materials with controlled and narrow particle size distribution.[9–12] The process also enables very efficient powder morphology control and the use of relatively cheap precursors. The precursors also have great potential as efficient solutions for the synthesis of various metal powders, among which copper powders have a special place. In the USP process, an aqueous metal–ion solution is atomized into the corresponding aerosol. This aerosol is then transported by a carrier gas into a hot reactor, where the aerosol droplets undergo drying, droplet shrinkage, solute precipitation, thermolysis, and sintering. Very short residence time, frequently less than 1 minute, is generally long enough to ensure the formation of desired spherical nanoproducts.

In this article, the well-known Lang equation/model was compared with obviously more comprehensive model of Jokanović *et al.*,[13–15] which in contrast to other models, given in literature, includes many additional parameters, such as particle diameter size distribution,

VUKOMAN JOKANOVIĆ, Research Professor, and BOŽANA ČOLOVIĆ, Research Associate, are with the Institute of Nuclear Sciences "Vinča", University of Belgrade, 11001 Belgrade, Serbia. Contact e-mail: vukoman@vinca.rs SREĆKO STOPIĆ and BERND FRIEDRICH, Research Professors, are with the IME Process Metallurgy and Metal Recycling, RWTH Aachen University, 57410 Aachen, Germany.

as well as subparticle diameters and the frequency of their appearance. In this article, both models were also compared with the corresponding experimental data for Cu powders, synthesized from precursor solutions of different concentrations. Therefore, the main aim of these investigations was not only to synthesize nano-structured Cu particles of well-defined morphology but also to try to predict as accurately as possible their size distribution by capillary break up waves model given by Jokanović et al.[15]

In agreement with our previous investigations, particle design related to this model includes all particle structural levels, and therefore, it is of exceptional importance for theoretical predictions of particle size distributions, their design, and subdesign, successfully made for various systems as reported in several articles.[10,15–17]

This approach developed for a number materials is quite original and creates the possibility to produce copper powders in advance of required particle size distribution characteristics. In addition, to the best of our knowledge, this approach by the first time is applied for copper powders obtained by USP.

II. EXPERIMENTAL

A. Material and Procedure

Copper sulfate ($CuSO_4 \cdot 5H_2O$; Merck, Darmstadt, Germany) was used as a precursor for the synthesis of copper powder by ultrasonic spray pyrolysis, carried out in a USP setup composed of an ultrasonic atomizer, a reactor with three separated heating zones, and an electrostatic precipitator. The temperature and pressure were controlled using a thermostat and a vacuum pump. The atomization of the copper sulfate solution took place in the ultrasonic atomizer (Gapusol 9001; RBI, Meylan, France) with a transducer to produce the aerosol. In accordance with our previous investigations,[9–12] the resonant frequency was selected to be 2.5 MHz.

In this setup, nitrogen was flushed from a separate bottle to remove air from the system. After that, hydrogen, as a reduction gas, was passed continuously through a quartz tube ($l = 1.5$ m, $b = 42$ mm) at a flow rate of 5 L/min. The atomized droplets of copper sulfate in an ultrasonic generator were then transported by hydrogen, as a carrier gas, inside a furnace.[6] After hydrogen reduction of the copper powder in the furnace, the obtained nanopowder was collected on the surface of an electrostatic collector (high-voltage device produced by Eltex, Elektrostatik-GmbH, Weil am Rhein, Germany).[7]

A scanning electron microscope (SEM) (ZEISS DSM 962, 1994; Carl Zeiss, Oberkochen, Germany) with a W-cathode (lateral resolution 2.5 nm at 30 kV) was used for characterization of the obtained copper powders. SEM images were used to observe the surface morphology of the particles formed at different parameter sets. The impurity level was determined by energy-dispersive spectroscopy analysis with an Si(Bi) X-ray detector, connected with the SEM and a multichannel analyzer. To prevent a possible cooper oxidation before SEM measurements, all samples were stored in small containers with volume only several times higher than powders volume and sealed by parafilm.

III. RESULTS AND DISCUSSION

A. Theoretical Model of Particle Size Design by Lang

The generation of the cloud of droplets by ultrasonic waves was studied by many researchers.[18,19] One of the most important approaches to estimate the mean size of aerosol droplets, obtained by USP, is given by the well-known Lang equation

$$d = 0.34 \cdot \left(\frac{8 \cdot \pi \cdot \sigma}{\rho \cdot f^2} \right)^{1/3} \quad [1]$$

where σ is the surface tension, ρ is the density of the atomized solution, and f is the frequency of an ultrasonic wave. In this equation, 0.34 is an empirical Lang's constant, obtained from the corresponding fitted data of his droplet measurements.

Assuming that the surface tension and density of the precursor solution can be approximately taken to be the same as those for water, e.g., $\sigma = 72.9 \times 10^{-3}$ Nm^{-1} and $\rho = 1.0$ g cm^{-3}, respectively, and using the experimental frequency value of 2.5 MHz, the theoretically predicted mean diameter of aerosol droplets by using Lang formula is 2.28 μm. This value is used for the mean particle diameter calculations. Assuming that each droplet is transformed into one particle only and that the coalescence or disintegration during atomization can be neglected, the final particle diameter is calculated by using the Messing equation[20]

$$D_p = d \cdot \left(\frac{C_p \cdot M_{Cu}}{\rho_{Cu} \cdot M_p} \right)^{1/3} \quad [2]$$

where D_p is the mean aerosol particle diameter, d is the mean droplet diameter, M_p and C_p are the molar mass and the concentration of the precursor solution, M_{Cu} is the copper molar mass, and ρ_{Cu} is the copper density.

In agreement with the Messing equation, using the parameters of our experiments (d: 2.28 μm, M_{Cu}: 63.55 g/mol, and ρ_{Cu}: 8.960 g/cm^3) and the concentration values of used copper sulfate solutions (0.05, 0.1, 0.3, 0.51, 0.6, and 1.18 mol/L), the corresponding mean copper particle diameters were calculated. The obtained values are: 152, 193, 245, 333, 352, and 442 nm, respectively.

It is obvious that according to the explanation offered briefly in Section I for the mechanism of particle solidification and the corresponding conditions that favor the given mechanism, different precursor solution concentrations may cause different mechanisms of droplet precipitation. In agreement with this, the shrinkage of droplets caused by solvent evaporation, salt conversion into metal by hydrogen reduction, and the formation and sintering of solid particles can have different rates and efficiencies, causing finally different degrees of particle volume reduction.

B. Our Approach to the Theoretical Modeling of Particle Design

1. Droplet and particle size prediction

The theoretical background for droplet and particle size predictions is given in more detail in our previous papers.[15–17] In this paragraph, only equations essential for the calculation of various structural parameters of Cu precursor are given. The first of the applied equations is equation Eq. [3], which describes the distribution of Cu-precursor droplet diameters, important for subsequent calculation of the Cu particle size distribution

$$d_n = \frac{1}{\pi}\left(\frac{2\sigma\pi}{\rho f^2}\right)^{\frac{1}{3}}[l(l-1)(l+2)]^{\frac{1}{3}} \qquad [3]$$

where d_n is the diameter of an aerosol droplet, σ is the surface tension of precursor, ρ is the density of precursor, f is the frequency of ultrasonic atomizer, and l is an integer, $l \geq 2$.

To obtain each discrete particle diameter value, Eq. [4] was used

$$I_{01} : I_{02} : \ldots : I_{0N} = \frac{1}{\Delta f_1} : \frac{1}{\Delta f_2} : \ldots : \frac{1}{\Delta f_n} \qquad [4]$$

where I_{01}, I_{02}, I_{0N} are the frequencies of appearance of the corresponding discrete values of diameters within a given range, whereas Δf_1, Δf_2,…,Δf_n represent the difference between the values of shifted frequencies within the terms related to the damping factor with respect to the excitation frequency of the ultrasonic oscillator. Assuming that the total contribution of all the fractions that make up the size distribution of discrete values of particle diameters is equal to one, the normalization of particles partition is done using Eq. [5]

$$I_{01} + I_{02} + \ldots + I_{0N} = 1 \qquad [5]$$

Equations [2] and [4] enable quantitative determination of contributions of all discrete diameter values of Cu precursor droplets and subsequently Cu particles.

In this way, the resulting pairs of values (discrete values given by Eqs. [2] and [3] and their individual contributions given by Eqs. [4] and [5]) provide a complete picture of the particle distribution in the system (they fully define the spectrum of particle size distribution within the system).

2. Model prediction and experimental data

The experimental mean diameters of Cu particles (d_{ap}) were obtained from Eq. [6]

$$d_{ap} = \frac{\sum_{i=1}^{n} n_i d_i}{\sum_{i=1}^{n} n_i} \qquad [6]$$

where n_i is a fraction of particles and d_i its diameter. By measuring particle diameters (the diameters of approximately 200 particles were measured from SEM images, Figures 1(a) through (c)), it was found that the mean diameters of particles were: 230, 290, 460, 560, 580, and 710 nm, for Cu samples obtained from the precursor of 0.05, 0.1, 0.3, 0.51, 0.6, and 1.18 mol/L concentration,

respectively. Their corresponding ranges of distribution were: 210 to 320 nm, 240 to 390 nm, 260 to 960 nm, 290 to 800 nm, 270 to 800, and 500 to 1020 nm, respectively. Between 80 pct and 90 pct of the particles were in the range of 210 to 240 nm ($c = 0.05$ mol/L), 240 to 290 nm ($c = 0.1$ mol/L), 260 to 560 nm ($c = 0.3$ mol/L), 400 to 690 nm ($c = 0.51$ mol/L), 400 to 740 nm ($c = 0.6$ mol/L), and 530 to 820 nm ($c = 1.18$ mol/L).

Experimental particle-size distribution data, expressed via particle diameters, for all precursor concentrations are statistically compared by using average diameter value, maximum and minimal diameter value, distribution range, and relative deviation. All these values are given in Figure 1 and Table I. From these data, particularly those for relative deviation, it is obvious that the diameter values are spread out/scattered over a wide range of values (the lowest relative deviation was 16 pct and the highest was 42 pct).

Besides this simple statistics analysis, the particle diameter distribution data, for all precursor concentrations, can be obtained by comparing the data for experimental particle distribution with those obtained by fitting these data to the Gaussian and the Lorenz curve for probability distribution (Table II).

The sum of squared residuals (RSS), (RSS $= \sum_{i=1}^{n}(y_i - f(x_i))^2$, where y_i is the ith value of the variable to be predicted, x_i is the ith value of the explanatory variable, and $f(x_i)$ is the predicted value of y_i) is chosen as a comparing parameter because it is a measure of the discrepancy between the experimental data and applied distribution functions (Gaussian and Lorenz). Therefore, it follows that small RSS indicates a tight fit of the model to the given data. In our case, both curves (Gaussian and Lorenz) gave the best fit to diameter data for the precursor concentration of 0.05 mol/L (RSS calculated for fitting to the Gaussian function was 0.00038 and to the Lorenz function 0.00043), whereas the worst fit was obtained for diameter data with the highest RSS value (0.0434 the Gaussian and 0.0434 the Lorenz function), which was gathered for the precursor concentration of 0.6 mol/L (Table II). A very good fit for both distribution curves (Gaussian and Lorenz) was obtained only for the precursor concentration of 0.05 mol/L, whereas the fitting for the concentration of 0.6 mol/L was fairly satisfactory. For all other precursor concentrations, the fitting was unsatisfactory. The most unsatisfactory fitting was obtained for precursor concentrations of 0.1 and 0.51 mol/L. For precursor concentration $c = 0.3$ mol/L, the Gaussian curve fitting was completely unsatisfactory, whereas the Lorenz curve fitting was slightly better. From the analysis of RCS, the same conclusions can be drawn.

For theoretical prediction of droplet and particle sizes following the given model, Eq. [3] was used, whereas Eqs. [4] and [5] were applied for the determination of their partitions.
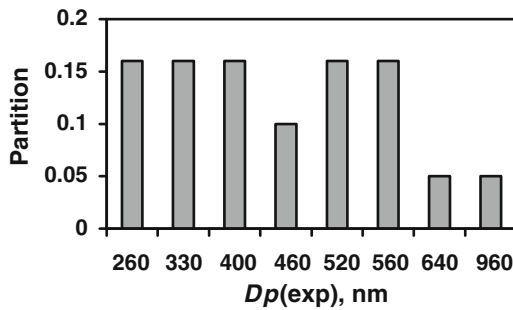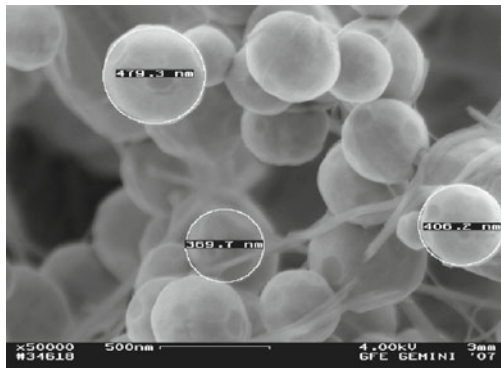
According to the model, the calculated droplet diameters are in the range 2.5 to 7.97 μm (the set of obtained values is as follows: 2.56, 3.97, 5.3, 6.6, and 7.97 μm, and their corresponding partition values 0.23, 0.34, 0.17, 0.14, and 0.12, obtained by using Eqs. [4] and [5]).
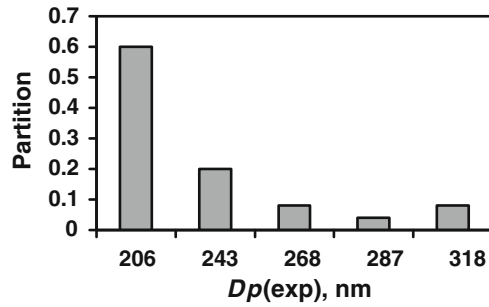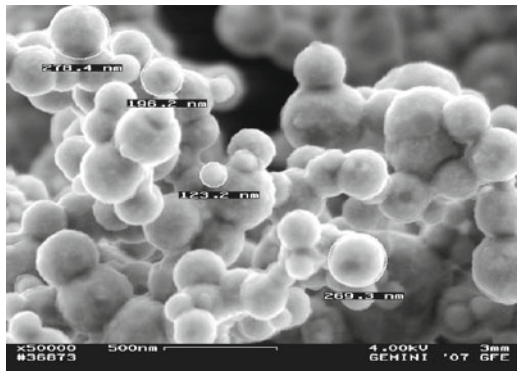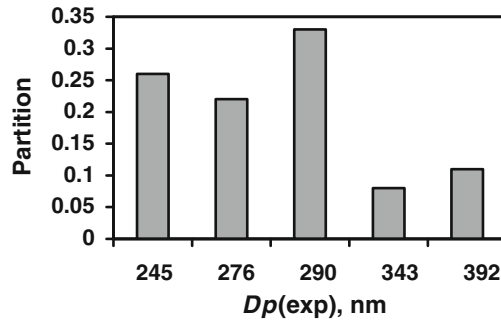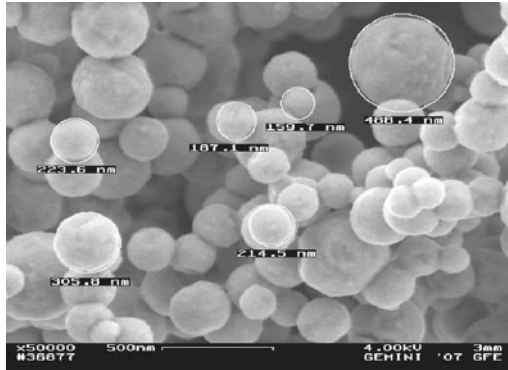
Fig. 1—Typical appearance and distribution of Cu particles obtained by USP at 1173 K (900 °C) for various concentrations of CuSO₄: (*a*) $c = 0.05$ mol/L, (*b*) $c = 0.1$ mol/L; (*c*) $c = 0.3$ mol/L; (*d*) $c = 0.51$ mol/L, (*e*) $c = 0.6$ mol/L, and (*f*) $c = 1.18$ mol/L.

Applying Eq. [3], the values of particle diameters, obtained by our model, are distributed between 139 and 432 nm for the precursor concentration 0.05 mol/L, 175 and 547 nm for the concentration 0.1 mol/L, 233 and 728 nm for the concentration 0.3 mol/L, 301 and 931 nm for concentration 0.51 mol/L, 314 and 977 nm for concentration 0.6 mol/L, and between 393 and 1246 nm for concentration 1.18 mol/L (Figure 2).

The mean diameters of Cu particles, calculated by our model (using Eqs. [3] through [5]), are 258 nm (precursor concentration $c = 0.05$ mol/L), 322 nm ($c = 0.1$ mol/L), 430 nm ($c = 0.3$ mol/L), 553 nm ($c = 0.51$ mol/L), 579 nm ($c = 0.6$ mol/L), and 725 nm ($c = 1.18$ mol/L)

showing fairly good agreement with the corresponding experimental values (Figure 2). Moreover, in both cases, the distribution is similar and narrow.

In an analysis of theoretical predictions of average particle diameters, the data obtained by using our model were compared with the corresponding data obtained by using the well-known Lange equation and with the experimental diameter data, obtained for all investigated precursor concentrations. The prediction of average particle diameters according to the Lange equation gives a set of values, given in Section III–A. A very high degree of discrepancies, between these and experimentally obtained data (from 33.4 pct, for the precursor
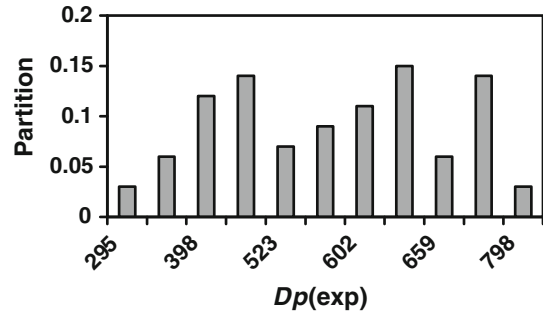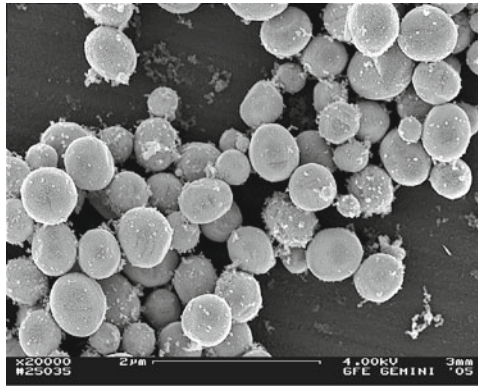
(d)
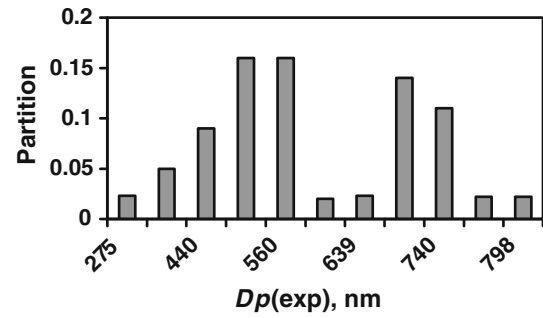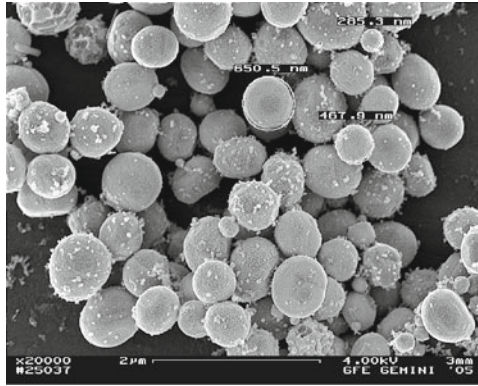
(e)
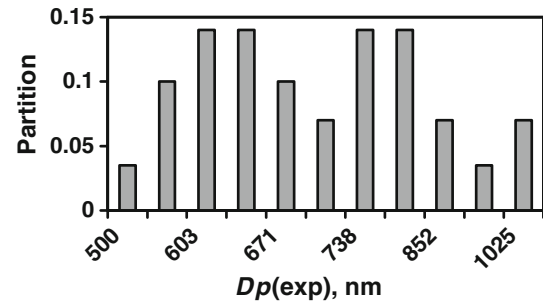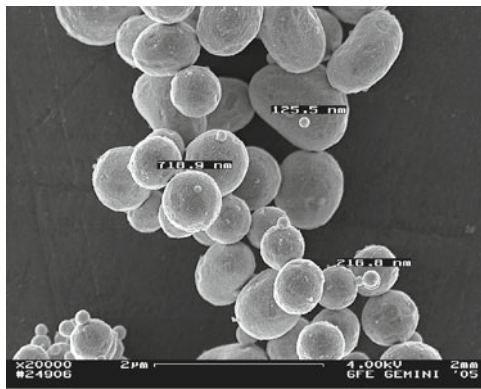
(f)

Fig. 1—Continued.

Table I. Average Diameter Value: Experimental (d_{av}), Jokanović d_{avJ}, Lange d_{avL}, Relative Deviation Values ρ Calculated in Agreement to Jokanović and Lange ($\rho = [d_{av} - d_{av}(exp)]/d_{av}(exp)$; $d_{av} = d_{avJ}$ or d_{avL})

c (mol/L)	d_{av}(exp) (nm)	d_{avJ} (Jokanović) (nm)	D_{avL}(Lange) (nm)	ρ($d_{Jokanovic}$) (pct)	ρ(d_{Lange}) (pct)
0.05	230	258	152	12	34
0.1	290	322	193	11	33
0.3	460	430	245	6.3	47
0.51	560	553	333	0.7	40
0.6	580	579	352	0.9	40
1.18	710	725	442	1.8	38

Table II. The Statistical Parameters, Obtained by Fitting Experimental Data to the Gaussian and the Lorenz Curve

c (mol/L)	RSS (G)	RCS (G)	RSS (L)	RCS (L)
0.05	0.000379	0.000379	0.000431	0.000431
0.1	0.0434	0.0434	0.0434	0.0434
0.3	0.018	0.0045	0.00442	0.0011
0.51	0.01091	0.00156	0.01092	0.00156
0.6	0.01908	0.00273	0.01845	0.00264
1.18	0.00866	0.00124	0.00865	0.00124

RCS: reduced chi-square; RSS: sum of squared residuals.

concentration of 0.05 mol/L, to 46.6 pct, for the precursor concentration of 0.3 mol/L) is observed.

In contrast, the data obtained using our model for the prediction of average diameter values showed a much better fit to experimental data, for any given precursor concentration. The maximal deviation from the experimental value was 11.7 pct for the lowest precursor concentration of 0.05 mol/L, whereas in some cases (precursor concentrations of 0.51 and 0.6 mol/l), the deviations were almost negligible (0.007 pct and 0.008 pct). The highest deviation can be attributed to very low precursor concentrations, which can cause partial droplet disintegration during their very fast heating inside of the furnace tube, as shown in Figure 3. These very low diameter values were excluded from the obtained experimental particle diameters (these values corresponding to precursor concentrations of 0.05 and 0.1 mol/l give diameters less than 180 nm), which were probably generated by droplet exploding into several independent fragments. This may be the reason for such a high discrepancy between the average diameters obtained experimentally and those predicted theoretically, using our model for precursor concentrations 0.05 and 0.1 mol/L (11.7 pct and 11 pct).

For higher precursor concentrations (0.3 to 1.18 mol/L), excellent agreement between theoretical and experimental data is evident. It seems that in these cases, the droplet disintegration by their exploding did not occur.

According to Figure 4, the discrepancy between the values obtained by Lang's equation and the experimental ones is considerable (in the range from 33.4 pct to 46.6 pct; in all cases, they are lower than appropriate experimental values, and in the inset at the upper left-hand corner of Figure 4, they are signed as [–]), whereas the discrepancy between the values obtained using our model and those obtained experimentally is much smaller, in the range from 0.007 pct to 11.7 pct. These values are in some cases a little bit higher, whereas in other cases, the values a little bit lower than the experimental ones (in a small additional figure at the left-hand corner of Figure 4 they are signed as [+] or [–]).

Finally, the relationship between average particle sizes and precursor concentrations, as it is shown in Figure 5, gives a parabolic function with a high degree of fitting to the corresponding experimental data. Therefore, by applying appropriate equation (which describes this function), it was possible to calculate the average diameters from corresponding precursor concentrations. This proves that it is possible to create precursor concentration for any requested average particle diameter. This fact is of great practical importance from the aspect of requested design of such kind of experiments.

3. *Mechanism of droplets precipitation and consequences*

According to many reports, the way of precipitation (volume, which gives a dense particle after full precipitation or surface, which gives particles as hollow spheres or rings, or porous particles) in a given system depends on various parameters, like solution supersaturation, temperature coefficient of precursor solubility, degree of solubility and temperature of melting of precursor salts, their three-dimensional networking, etc.[15,17,20]

In agreement, for a volume precipitation (which gives dense particles) to occur, it is necessary to have a precursor-solute with the following properties:

(a) Large difference between solute critical supersaturation and equilibrium saturation (in our case the precursor concentration was between 0.006 [the lowest] and 0.14 [the highest] of the concentration of saturation of $CuSO_4 \cdot 5H_2O$ at 373 K [100 °C]).
(b) High solubility and positive temperature coefficient to satisfy the percoloration criteria (thermal coefficient of solubility of $CuSO_4 \cdot 5H_2O$ shows positive value [0.8 °C^{-1}])
(c) Thermoplasticity or melting during the thermolysis stage of USP (melting point of $CuSO_4 \cdot 5H_2O$ – 373 K [110 °C]) should be neglected
(d) Colloid solutions and a partially hydrolyzed alkoxide system, which can very easily form three-dimensional networks by gelling or polymerization, are preferentially volume precipitated.

According to literature, it is obvious that our precursor fulfills the above given criteria. The concentrations of $CuSO_4 \cdot 5H_2O$ precursor between 0.006 (the lowest) and 0.14 (the highest) compared with the saturated solution concentration at 373 K [100 °C]) show that the concentrations are far below the solubility level. Great differences in $CuSO_4 \cdot 5H_2O$ solubility at 20 K and 373 K (100 °C) (approximately six times), and positive thermal coefficient of solubility (0.8 °C^{-1}) show that criteria (a) and (b) are fulfilled. After completing the process of droplets precipitation on its surface, the temperatures inside of this very thin layer rise rapidly, whereas the temperature inside droplets volume remains 383 K (100 °C), until the water completely evaporates. This process causes a rapid increase in the surface temperature
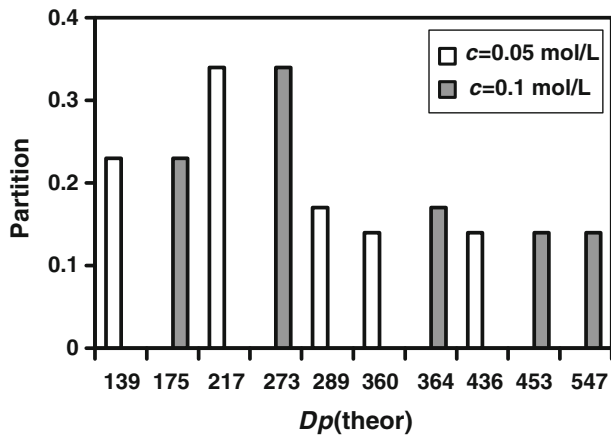
(a)
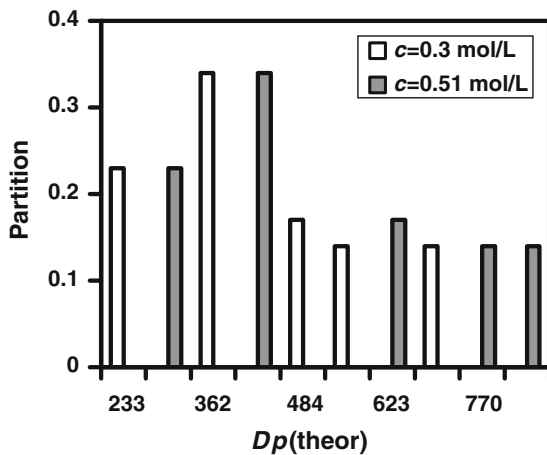
(b)
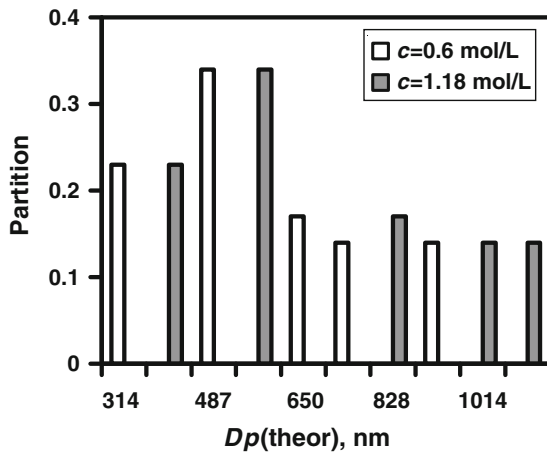
(c)

Fig. 2—Diagram of theoretical particle diameters for various precursor concentrations: (*a*) *c* = 0.05 and *c* = 0.1 mol/L; (*b*) *c* = 0.3 and *c* = 0.51 mol/L, and (*c*) *c* = 0.6 and 1.18 mol/L, obtained by our model.
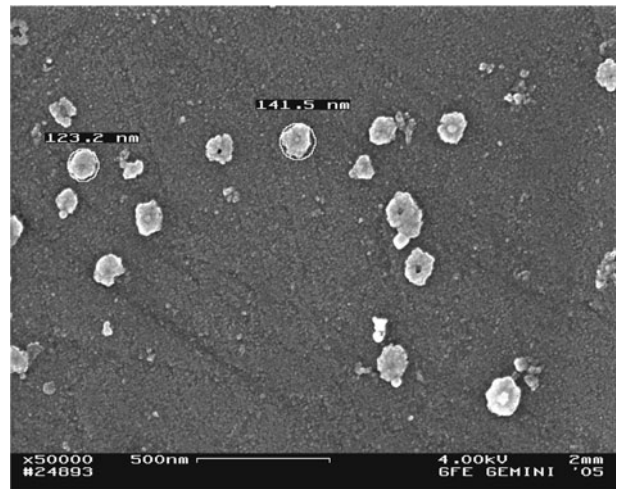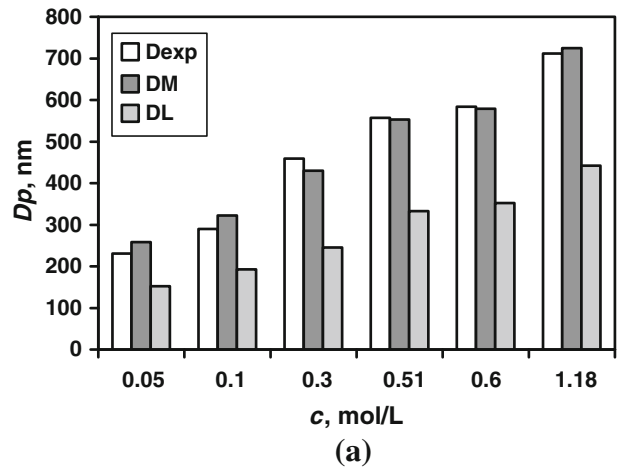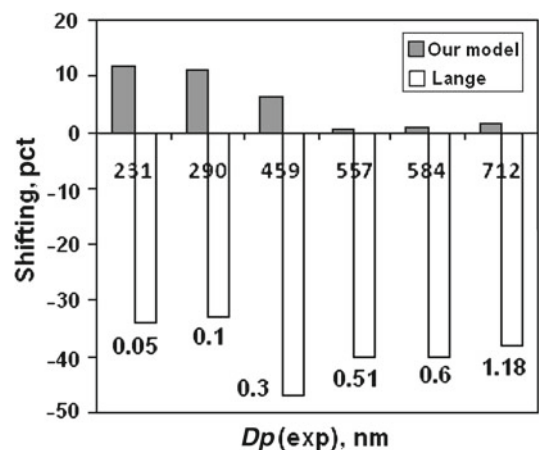

Fig. 3—The typical appearance of small fragments of particles obtained as a consequence of droplet disintegration for precursor concentrations 0.05 and 0.1 mol/L.

(a)

(b)

Fig. 4—(*a*) Average particle diameters for various precursor concentrations, obtained from experimental data-D_{exp}, our model-D_M and Lang formula. (*b*) A shift in average values obtained by our model and Lange formula from average experimental data.
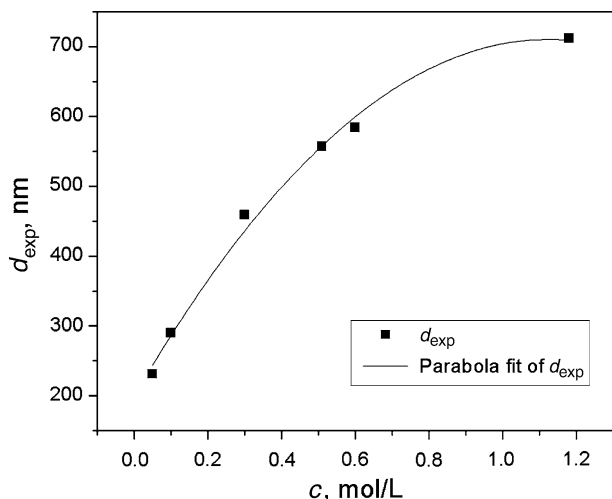
of the droplets to the value of the melting point of $CuSO_4 \cdot 5H_2O$ salt (the melting temperature of $CuSO_4 \cdot 5H_2O$ at 383 K [110 °C] is slightly higher than that of boiling water). Therefore, diffusion of the remained

Fig. 5—The relationship between average particle sizes and precursor concentration.

solutions, followed by hydrogen reduction, was shown to be a suitable method for the synthesis of spherical, nonagglomerated, and uniform nanopowders of copper with particle sizes $d = 230$ to 710 nm.

The use of Jokanović and coworkers' model allows the estimation of mean Cu particle sizes as well as characteristic parameters of Cu powder synthesis, such as the frequency of droplet formation and the difference between this frequency and forced frequency of ultrasonic generator. The mean theoretical diameters of Cu particles obtained by the model were 258, 322, 430, 553, 579, and 725 nm for precursor concentration of 0.05, 0.1, 0.3, 0.51, 0.6, and 1.18 mol/L, respectively. This is in good agreement with experimental mean particle diameter values 230, 290, 460, 560, 590, and 710 nm, respectively. In comparison with the Lang model, this model showed significantly better agreement with the measured diameter data.

water in droplet becomes more difficult, causing the deformation and potential breaking of the particles generated from these droplets.

In agreement with this, a difference between solution supersaturation and equilibrium saturation arises with increased difference temperature on the surface droplets and inside of their volume, during the heating inside of the furnace. Also, it is known, in thermochemistry, that copper sulfate pentahydrate decomposes at 336 K (63 °C) by releasing two water molecules and two additional ones at 382 K (109 °C). Finally, the last remained water molecule releases at 493 K (220 °C). In this way, the final product of salt dehydration becomes $CuSO_4$ anhydrite, which decomposes into CuO and SO_3 at 923 K (650 °C), without previous melting between 383 K and 423 K (110 °C and 150 °C).[21] Finally, CuO is hydrogen reduced to convert into Cu powders.

From these facts, clearly shown in preceding short explanation, the main conditions, which have to be fulfilled to enable volume precipitation of a precursor and to yield dense particles, are, more or less, satisfactory for all used $CuSO_4 \cdot 5H_2O$ concentrations (0.05, 0.1, 0.3, 0.51, 0.6, and 1.18 mol/L). For the lowest concentrations of $CuSO_4 \cdot 5H_2O$ (0.05 and 0.1 mol/L) and larger droplet diameters, partial surface droplet precipitation is also possible. This is influenced by a relatively high fraction of water compared with the fraction of dissolved precursor inside of such droplets.

These evidences are supported by very good agreement between theoretically obtained particle diameter values by using our model (which assumes dense particles as final products) and the experimentally obtained ones.

IV. CONCLUSIONS

The USP is a very promising method for the preparation of nanosized copper particles. USP of various Cu

REFERENCES

1. A. Owais and B. Friedrich: *Erzmetall*, 2003, vol. 56, pp. 668–78.
2. E. Jäskeläinen, O. Hyvärinen, and M. Hämäläinen: *Pressure Hydrometallurgy*, M.J. Collins and V.G. Papangelakis, eds., Canadian Institute of Mining, Metallurgy, and Petroleum, Montréal, Cananda, 2004, pp. 119–25.
3. Y. Champion, F. Bernard, N. Guigue-Millot, and P. Perriat: *Mater. Sci. Eng. A*, 2003, vol. 360, pp. 258–63.
4. G. Vitulli, M. Bernini, S. Bertozzi, E. Pitzalis, P. Salvadori, S. Coluccia, and G. Martra: *Chem. Mater.*, 2002, vol. 14, pp. 1183–90.
5. T. Chen, L.N. Zhang, and H. Lu: *J. Phys. Chem. B*, 2002, vol. 106, pp. 9017–22.
6. R.D. Rieke, W.R. Klein, and T.C. Wu: *Tetrahedron*, 1989, vol. 45, pp. 443–54.
7. A.A. Ponce and K.J. Klabunde: *J. Mol. Cat. A*, 2005, vol. 225, pp. 1–6.
8. S. Park, R.J. Gorte, and J.M. Vohs: *App. Cat. A*, 2000, vol. 200, pp. 55–61.
9. S. Stopic, S. Gürmen, and B. Friedrich: *J. Metall.*, 2005, vol. 11, pp. 65–73.
10. V. Jokanovic, B. Jokanovic, J. Nedeljkovic, and O. Milosevic: *Surf. Coll. A*, 2004, vol. 249, pp. 111–13.
11. S. Stopic, P. Dvorak, and B. Friedrich: *Metall*, 2006, vol. 60, pp. 377–82.
12. S. Gürmen, S. Stopic, and B. Friedrich: *Mater. Res. Bull.*, 2006, vol. 41, pp. 1882–90.
13. J.H. Kim, V. Babushok, T. Germer, G. Mulholland, and S. Ehrmann: *J. Mater. Res.*, 2003, vol. 18, pp. 1614–22.
14. S. Stopic, P. Dvorak, and B. Friedrich: *Erzmetall World Metall.*, 2005, vol. 58, pp. 195–98.

15. V. Jokanović, D.J. Janackovic, A. Spasic, and D. Uskokovic: *Mater. Trans. JIM*, 1996, vol. 37, pp. 627–35.
16. V. Jokanović, A.M. Spasic, and D. Uskokovic: *J. Colloid Interface Sci.*, 2004, vol. 278, pp. 342–52 .
17. V. Jokanović: *Finely Dispersed Particles: Micro-, Nano-, Atto-Engineering*, A.M. Spasic and J.P. Hsu, eds., CRC, Taylor & Francis, Inc. New York, NY, 2006, pp. 513–33.
18. R. Peskin and R. Raco: *J. Acoust. Soc. Am.*, 1963, vol. 33, pp. 1378–85.
19. F. Barreras, H. Amaveda, and A. Lozano: *Exp. Fluids*, 2002, vol. 33, pp. 405–13.
20. G.L. Messing, S.C. Zhang, and G.V. Jayanthi: *J. Am. Ceram. Soc.*, 1993, vol. 76, pp. 2707–26.
21. A.F. Holleman and E. Wiberg: *Inorganic Chemistry*, Academic Press, San Diego, CA, 2001, pp. 320–21.